J Materiomics 4 (2018) 56–61

Contents lists available at ScienceDirect

J Materiomics

journal homepage: www.journals.elsevier.com/journal-of-materiomics/

Structural evolution and reaction mechanism of lithium nickelate ($LiNiO_2$) during the carbonation reaction

Daniela González-Varela [a], Brenda Alcántar-Vázquez [b], Heriberto Pfeiffer [a, *]

[a] Laboratorio de Fisicoquímica y Reactividad de Superficies (LaFReS), Instituto de Investigaciones en Materiales, Universidad Nacional Autónoma de México, Circuito exterior s/n, CU, Del. Coyoacán, CP 04510, Ciudad de México, Mexico

[b] Instituto de Ingeniería, Coordinación de Ingeniería Ambiental, Universidad Nacional Autónoma de México, Circuito Escolar s/n, CU, Del. Coyoacán, CP 04510, Ciudad de México, Mexico

ARTICLE INFO

Article history:
Received 11 September 2017
Received in revised form
6 December 2017
Accepted 20 December 2017
Available online 21 December 2017

Keywords:
Lithium nickelate
CO_2 chemisorption
Lithium diffusion coefficient
Phase transition

ABSTRACT

Lithium nickelate ($LiNiO_2$) was synthesized using the lithium excess method, and then characterized by X-ray diffraction, scanning electron microscopy and N_2 adsorption-desorption. Finally, differential thermal and thermogravimetric analyses were performed in CO_2 presence, at high temperatures. Results show that $LiNiO_2$ is able to react with CO_2 through a complex structural evolution process, where lithium atoms are released to produce Li_2CO_3, while some nickel atoms are rearranged on different $Li_{1-x}Ni_{1+x}O_2$ crystalline phases. $LiNiO_2$-CO_2 reaction kinetic parameters were determined assuming a first-order reaction, where kinetic constants tended to increase as a function of temperature. However, kinetic constant values did not follow a linear trend. This atypical behavior was attributed to $LiNiO_2$ sintering and crystalline evolution performed as a function of temperature.

© 2018 The Chinese Ceramic Society. Production and hosting by Elsevier B.V. This is an open access article under the CC BY-NC-ND license (http://creativecommons.org/licenses/by-nc-nd/4.0/).

1. Introduction

High temperature carbon dioxide (CO_2) sorbents have recently drawn significant interest, as direct CO_2 capture (in this temperature range, $T > 400\,^{\circ}C$) can improve energy efficiency by overcoming the gas cooling process to ambient temperature [1]. In this context, lithium-based ceramics such as Li_2ZrO_3 [2–5], $Li_6Zr_2O_7$ [6], Li_8SiO_6 [7,8], Li_5AlO_4 [9,10], Li_4SiO_4 [11–17] and Li_2CuO_2 [18–21] have been extensively studied as possible high temperature CO_2 captors, among other applications [22–26]. Moreover, some researchers have tried to improve their CO_2 capture properties developing different synthesis methods, modifying structural or microstructural characteristics and identifying the most appropriate operation conditions [7,13,25–32].

Other important applications of the high-temperature CO_2 sorbents are the sorption enhanced steam reforming (SESR) and the oxidation-capture of carbon monoxide in H_2-rich gas flows (eliminating CO from the reformed fuels) [1,33–38]. In the first case, very few theoretical and experimental studies have documented the application of alkaline ceramics such as Li_2ZrO_3, Li_4SiO_4, and Na_2ZrO_3 in the SESR of methane and ethanol, where in most of these cases the addition of another catalytic material is needed [1,33–38]. Also, some alkaline ceramics have been used cyclically in the carbonation and subsequent methane reforming processes [39] and last but not least, some of these ceramics have shown high CO_2 chemisorption even at low CO_2 partial pressures (P_{CO2} values between 0.2 and 0.05) [12,14,20], which is a closer CO_2 concentration than those present in real combustion gases.

On the contrary, CO oxidation process has been widely studied using different catalysts, such as noble or transition metals (Fe, Ni, Cu, Co) [40]. However, in the last year, some alkaline ceramics, as Na_2ZrO_3, $NaCoO_2$ and Li_2CuO_2, have been tested as bifunctional materials (CO oxidant catalyst and CO_2 captors), showing interesting CO conversions in wide temperature ranges [21,41,42].

Contrariwise, lithium nickelate ($LiNiO_2$) is widely used as attractive cathode material for rechargeable lithium batteries [43–45]. $LiNiO_2$ has a rhombohedral structure with trigonal symmetry (space group: *R-3m*), with two interpenetrating close-packed FCC sub-lattices: One sub-lattice containing oxygen ions, while the other contains Li and Ni cations, both alternating (111) planes [43]. $LiNiO_2$ synthesis has been developed using different techniques, such as hydrothermal decomposition, melt-impregnation, Pechini method, solid-state and sol-gel, among others [43,45].

* Corresponding author.
E-mail address: pfeiffer@iim.unam.mx (H. Pfeiffer).
Peer review under responsibility of The Chinese Ceramic Society.

https://doi.org/10.1016/j.jmat.2017.12.004
2352-8478/© 2018 The Chinese Ceramic Society. Production and hosting by Elsevier B.V. This is an open access article under the CC BY-NC-ND license (http://creativecommons.org/licenses/by-nc-nd/4.0/).

$LiNiO_2$ has interesting structural and diffusion characteristics. Thus, CO_2 chemisorption would be produced on $LiNiO_2$, as this crystalline structure might facilitate lithium diffusion and release processes towards CO_2 reactivity. Therefore, in the present work, the excess lithium method was used to synthesize lithium nickelate and its CO_2 capture properties were investigated by thermogravimetric analysis at different temperatures.

2. Experimental section

Lithium nickelate ($LiNiO_2$) was synthesized by lithium excess method. Initially, lithium hydroxide ($LiOH•H_2O$, Caledon) and nickel nitrate ($Ni(NO_3)_2•6H_2O$, Meyer) were dissolved in water, using a Li/Ni molar ratio equal to 4. This solution was mechanically mixed and heated to 80 °C till water was totally evaporated (~20 h). Resulting powder was calcined at 700 °C for 5 h in air [44].

Lithium nickelate was analyzed structural and microstructurally by X-ray diffraction (XRD), N_2 adsorption-desorption, scanning electron microscopy (SEM), thermogravimetric (TGA) and differential thermal (TDA) analyses. XRD patterns were obtained with a BRUKER AXS D8-Advance diffractometer coupled to a Cu anode X-ray tube. The K_α wavelength was selected with a diffracted beam monochromator, and compounds were identified conventionally using the PDF database. N_2 adsorption-desorption isotherm of the $LiNiO_2$ sample was obtained on a Bel-Japan Minisorp II instrument at 77 K, using a multipoint technique (N_2 from Praxair, grade 4.8). Prior to analysis, the sample was degassed at room temperature for 24 h. The surface area was determined using the Brunauer-Emmett-Teller (BET) method. Then, $LiNiO_2$ morphological characteristics were determined by SEM, using a JEOL JMS-7600F equipment. Finally, simultaneous thermogravimetric and differential thermal analyses were performed in SDT-Q600 TA Instruments equipment, from TA Instruments. $LiNiO_2$ was heat-treated, using a heating rate of 5 °C min^{-1} and a gas flow of 60 ml min^{-1}, from room temperature to 850 °C. These analyses were carried out on two different atmospheres: N_2 (Praxair, grade 4.8) and CO_2 (Praxair, grade 3.0).

The CO_2 chemisorption processes were evaluated in a thermobalance (TA Instruments, model Q500HR), using dynamic and isothermal conditions. Initially, $LiNiO_2$ was dynamically heated from 30 to 850 °C using a heating rate of 5 °C min^{-1}. $LiNiO_2$ isothermal experiments were performed by heating the sample to desired temperature (between 400 and 800 °C), under a N_2 flux. Then, the gas flow was switched from N_2 to CO_2. All these experiments were performed using a CO_2 flow of 60 ml min^{-1} (CO_2-Praxair, grade 3.0). Finally, isothermal products were re-characterized by XRD in order to identify CO_2 chemisorption mechanism on $LiNiO_2$.

3. Results and discussion

The XRD pattern, of $LiNiO_2$ synthesized using the lithium excess method, is shown in Fig. 1. As it can be seen, XRD pattern fitted to the 00-089-3601 PDF file, which corresponds to $LiNiO_2$. In addition, small amounts of Li_2CO_3 were detected (00-022-1141 PDF file). The formation of this secondary phase is in good agreement with synthesis method; lithium excess.

After the structural characterization, some microstructural characteristics of $LiNiO_2$ were analyzed by SEM and N_2 adsorption-desorption. Fig. 2 shows a backscattered electron image of $LiNiO_2$ particles. The morphology corresponded to agglomerates composed by irregular polyhedral particles of around 400–600 nm. This image shows the presence of two different compounds, by contrast, which must correspond to $LiNiO_2$ (bright and main phase) and very small amounts of Li_2CO_3 (dark phase), according to their differences in the mean atomic numbers ($\overline{Z}$) and backscattered

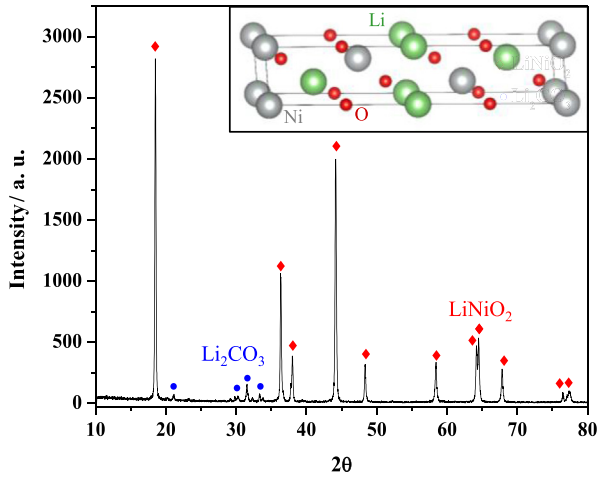

Fig. 1. XRD pattern and crystal structure of $LiNiO_2$ synthesized using the lithium excess method.

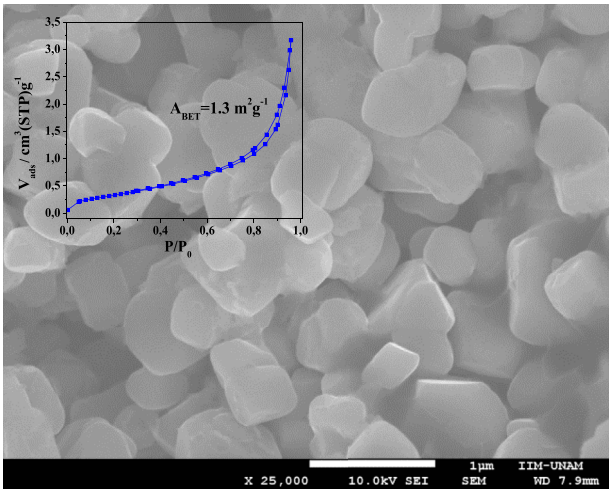

Fig. 2. Backscattered electron image of $LiNiO_2$ particles and N_2 adsorption–desorption isotherm (square inset).

electron coefficients (η); $LiNiO_2$ ($\overline{Z}$ = 11.75 and η = 0.138) and Li_2CO_3 ($\overline{Z}$ = 6 and η = 0.064). Additionally, N_2 adsorption-desorption analysis (square inset of Fig. 2) fits to type II isotherm without hysteresis, according to IUPAC classification, which corresponds to non-porous materials [46]. The $LiNiO_2$ surface area, calculated using BET model [46], was equal to 1.3 m^2 g^{1-}. All these microstructural features are in good agreement with the final heating process performed during $LiNiO_2$ synthesis, which must induce a ceramic sintering process, producing polyhedral particles with low surface area.

Different nickel compounds have been used as catalysts. Then, combination of this transition metal and lithium may propitiate some interesting physicochemical properties, such as its possible application on sorption enhance processes or bifunctional components, as it was described in the introduction section. Here, as an initial case of study, the CO_2 capture process was analyzed. It has to be pointed out that lithium availability on $LiNiO_2$ ($Li/Ni_{molar\ ratio}$ = 1) is not as high as in other alkaline ceramics, where Li/M (M = Si, Zr, Al or Cu, among others) molar ratio is equal or higher than two [7–11,16,21,32,47–50]. In this case, lithium nickelate may react with carbon dioxide according to the following reaction:

$$2\ LiNiO_2 + CO_2 \rightarrow Li_2CO_3 + Ni_2O_3 \quad (1)$$

Fig. 3 shows the $LiNiO_2$ dynamic curve in a CO_2 flow. Initially, $LiNiO_2$ exhibited a small mass decrease of 1 wt%, associated to superficial dehydration process. After that, the curve showed a non-continuous increase process, between 200 and 850 °C. Mass increment can be divided in three different temperature ranges; 200–390, 445–650 and 660–850 °C. Usually, CO_2 capture on lithium and sodium ceramics depicts only one or two different mass increments, which are associated to superficial and bulk CO_2 chemisorption processes [8,12,14,15,51–53]. However, in this case, $LiNiO_2$ presented a triple process. Therefore, different thermal analyses were performed to understand this atypical behavior. Fig. 4 shows the TG and DT analyses of $LiNiO_2$ into two different gas flows; N_2 or CO_2. When N_2 was used, dehydration process was observed in both curves (TG and DT at $T \leq 100$ °C), followed by a crystalline phase transformation registered at 410 °C by differential thermal analysis. After that, $LiNiO_2$ evidenced a decarbonation process, which is in good agreement with the Li_2CO_3 presence previously determined by XRD. As it could be expected, when CO_2 was used as flow gas, dehydration and crystalline phase transformation process were not as evident as in the previous case, although they are still visible. This effect must be related to CO_2 chemisorption produced in a wide temperature range. In any case, the variation observed during the CO_2 chemisorption in $LiNiO_2$ can be associated to a crystalline phase transformation.

Therefore, based in all previous results, there is an initial CO_2 superficial reaction between 200 and 390 °C. After that, the remaining $LiNiO_2$ suffers a crystalline phase transformation at 410 °C, which induces the second CO_2 chemisorption between 445 and 650 °C. $LiNiO_2$ phase transformation should induce diffusion of some lithium and/or oxygen atoms, promoting a second chemisorption process. Then, at temperatures between 660 and 850 °C the third and final CO_2 chemisorption is produced. This final process is related to bulk CO_2 chemisorption, where different diffusion processes must be activated. Something else must be pointed out; lithium ceramics usually traps CO_2 at $T \leq 720$ °C, as lithium carbonate decomposes at this temperature. Thus, CO_2 chemisorption-desorption equilibrium is modified at higher temperatures. In this case, CO_2 capture continued up to 850 °C, which is not usual situation. In a previous work [32], a similar behavior was observed when lithium orthosilicate (Li_4SiO_4) was doped with aluminum. In that case, $Li_{4+x}Si_{1-x}Al_xO_4$ solid solution was synthetized and it was able to chemisorb CO_2 from 250 to 800 °C. Those samples trapped

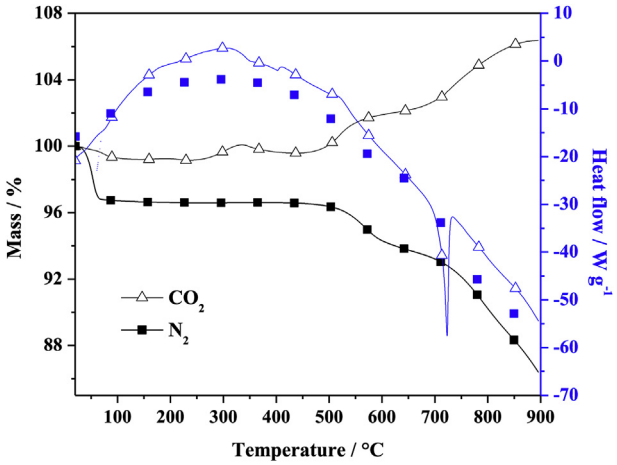

Fig. 4. TG (black) and DT (blue) analyses of $LiNiO_2$ into two different gas flows; N_2 or CO_2.

CO_2 at higher temperatures than 720 °C, due to high thermal stability and high lithium diffusion coefficient of a secondary phase ($LiAlO_2$), which modified the CO_2 chemisorption-desorption equilibrium. In the present case, a similar situation occurred due to $Li_{0.4}Ni_{1.6}O_2$ phase formation, as it is probed below (see XRD results of the CO_2 isothermal products).

After dynamic TG and DT analyses, different isotherms were performed, and the isothermal sample products were characterized by XRD to confirm CO_2 chemisorption, and to explain the high thermal stability, elucidating a possible reaction mechanism. Fig. 5 shows the $LiNiO_2$ isothermal graphs at different temperatures. At 400 °C, $LiNiO_2$ only captured 1.8 wt% and the isotherm did not reach the equilibrium. When temperature was increased between 500 and 700 °C (after the $LiNiO_2$ crystal phase transition determined by DTA), $LiNiO_2$ captured between 4.8 and 6.8 wt%. Finally, at 750 and 800 °C, the highest weight increments were observed, 11.3 and 11.8 wt %, respectively. In fact, these weight increments are around 50% of the maxima theoretical efficiency (22.5 wt%). This result is comparable to other experimental efficiencies obtained by lithium ceramics [3,8,9,13,18,19,48,54,55]. Moreover, $LiNiO_2$ carbonation stability was confirmed in these experiments, as CO_2 desorption was not evidenced, even at 800 °C.

All the isothermal sample products were analyzed structurally

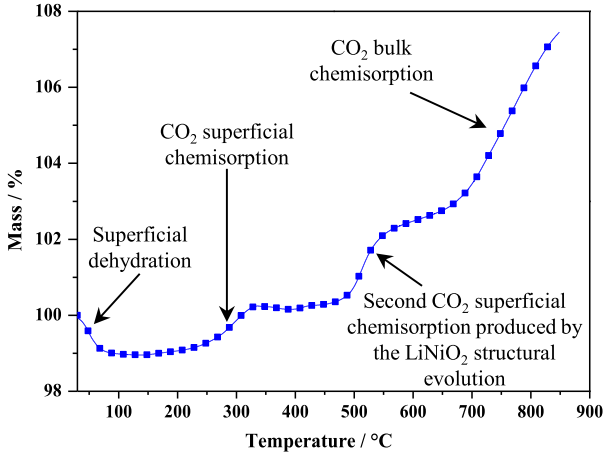

Fig. 3. Dynamic TG analysis of $LiNiO_2$ in a CO_2 flow, showing different thermal processes.

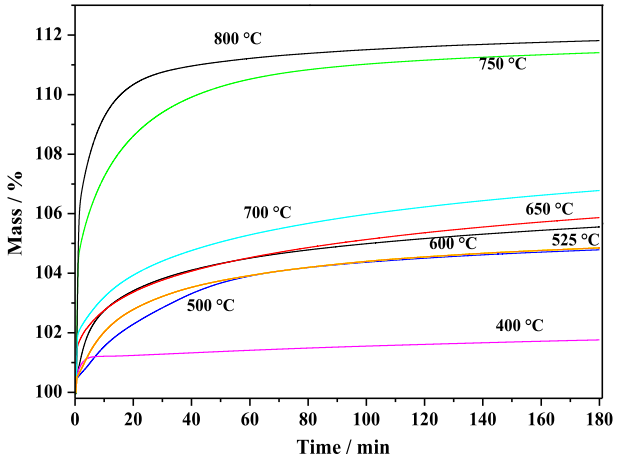

Fig. 5. $LiNiO_2$ isothermal analyses at temperatures between 400 and 800 °C in a CO_2 flow.

by XRD (Fig. 6). In the isothermal sample product of 400 °C, XRD pattern evidenced the formation of a non-stoichiometric crystalline phase, $Li_{0.95}Ni_{1.05}O_2$, in addition to Li_2CO_3. It seems that CO_2 reacted superficially with $LiNiO_2$, producing some lithium vacancies. Then, between 500 and 525 °C NiO phase is confirmed, in addition to Li_2CO_3, as it could be expected, while $Li_{0.95}Ni_{1.05}O_2$ phase tended to decrease. It must be mentioned that NiO diffraction peaks present a right shift, which may be associated to a crystalline cell parameters contraction. This effect may be attributed to vacancies and/or lithium atoms into NiO crystalline structure. On the isothermal sample products obtained at 600 and 700 °C, $Li_{0.92}Ni_{1.08}O_2$ and $Li_{0.79}Ni_{1.21}O_2$ phases appeared in addition to Li_2CO_3, while NiO tended to disappear. Finally, XRD patterns, from isotherms obtained at the highest temperatures (750 and 800 °C), showed the formation of Li_2CO_3 and a different lithium nickelate phase, $Li_{0.4}Ni_{1.6}O_2$.

Previous studies have shown that lithium nickelate is able to create lithium vacancies producing non-stoichiometric phases, where some Ni^{3+} atoms diffuse to lithium structural positions as Ni^{2+}, stabilizing a crystalline non-stoichiometric structure [43,45]. In this case, the carbonation process induces different lithium behaviors. At the lowest temperatures ($T \leq 600$ °C), it seems that most of carbonation process is produced with lithium located at $LiNiO_2$ surface, resulting in NiO and Li_2CO_3. The rest of the lithium nickelate stands as $Li_{0.95}Ni_{1.05}O_2$, with only small crystalline modifications. In such a case, reaction must follow the next process, where the some nickel atoms are partially reduced and some oxygen atoms are released. At $T \geq 600$ °C diffusion processes are activated [32,51], inducing a different carbonation-reaction mechanism. In this temperature range, lithium atoms can diffuse and release from $LiNiO_2$, generating vacancies and consequently a lithium nickelate recrystallization process. Therefore, the carbonation-reaction mechanism, at high temperatures, can be described as follows:

$$2LiNiO_2 + \frac{1+x}{2}CO_2 \rightarrow Li_{1-x}Ni_{1+x}O_2 + \frac{1+x}{2}Li_2CO_3 + 1 - xNiO + \frac{1+x}{4}O_2 \quad (2)$$

Where the consecutive reaction process is:

$$2LiNiO_2 + 0.525CO_2 \rightarrow Li_{0.95}Ni_{1.05}O_2 + 0.525Li_2CO_3 + 0.95NiO + 0.2625O_2 \quad (3)$$

$$2Li_{0.95}Ni_{1.05}O_2 + 0.49CO_2 \rightarrow Li_{0.92}Ni_{1.08}O_2 + 0.49Li_2CO_3 + 1.02NiO + 0.245O_2 \quad (4)$$

$$2Li_{0.92}Ni_{1.08}O_2 + 0.525CO_2 + xNiO \rightarrow Li_{0.79}Ni_{1.21}O_2 + 0.525Li_2CO_3 + x\text{-}yNiO + xO_2 \quad (5)$$

$$2Li_{0.79}Ni_{1.21}O_2 + 0.59CO_2 + xNiO \rightarrow Li_{0.4}Ni_{1.6}O_2 + 0.59Li_2CO_3 + x\text{-}yNiO + xO_2 \quad (6)$$

In these reactions, y represents Ni^{2+} ions coming from the NiO crystalline structure, assuming that NiO acts as reagent in the whole reaction mechanism. This scheme would explain the NiO disappearance at high temperatures, where a final lithium nickelate structure is arranged; $Li_{0.4}Ni_{1.6}O_2$.

From this analysis, it can be established that there is a direct relationship between CO_2 capture and lithium nickelate non-stoichiometric phases produced after the carbonation process. Fig. 7 shows a comparative evolution of the CO_2 captured and lithium content in the nickelate product phase as a function of temperature. From this trend, it is clearly evident that $LiNiO_2$-CO_2 reaction process is highly dependent from lithium nickelate structural evolution, where lithium diffusion must be a critical issue.

Something else must be pointed out, CO_2 capture was not limited as a function of lithium content in the lithium nickelate phase evolution. It can be explained based in the temperature increment, but mainly due to lithium diffusion coefficients in the corresponding non-stoichiometric lithium nickelate phases. It has been reported that lithium diffusion coefficient ($\widetilde{D_{Li}}$) increases as a function of lithium vacancies [56]. For example, in the Li_xNiO_2 systems where the x value is equal to 0.92 and 0.6 the $\widetilde{D_{Li}}$ values are 7×10^{-9} and 4×10^{-8} cm^2/s, respectively. Therefore, CO_2 capture process is not limited through Li_xNiO_2 ceramic bulks, but the opposite.

To further analyze the curves presented in Fig. 5, data were fitted to a first-order reaction, as it has been reported for the CO_2 chemisorption in other alkaline ceramics [8,36,52,53]. As there are several processes involved in whole CO_2-$LiNiO_2$ reaction-mechanism, it can be assumed that a first-order reaction is taking place only during the first moments of CO_2 chemisorption. In such a case, the rate law can be described as:

$$\ln [LiNiO_2] = -kt \quad (7)$$

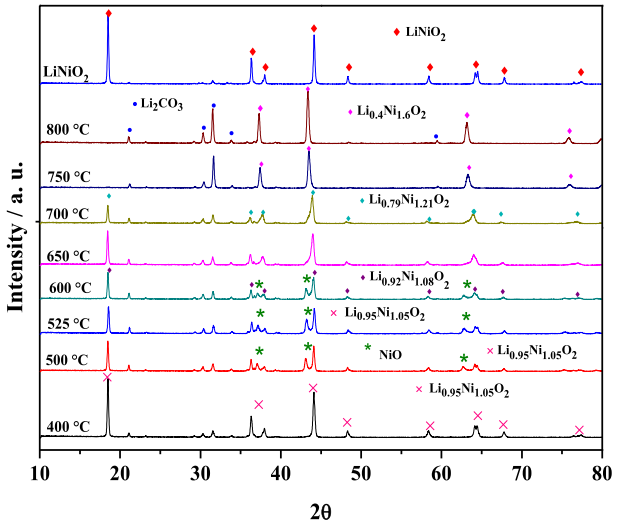

Fig. 6. XRD patterns of pristine $LiNiO_2$ and different CO_2 isothermal products.

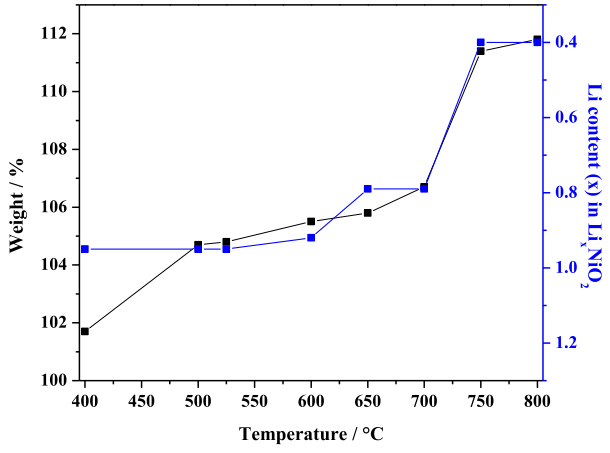

Fig. 7. Comparative evolution of CO_2 captured and lithium content on the remaining lithium nickelate structure as a function of temperature.

where, k is the reaction rate constant, t is time, and [$LiNiO_2$] is the molar concentration of lithium nickelate. Isotherms only fit linearly this model over very short intervals (~20 s). In that time, $LiNiO_2$ is reacting superficially with the CO_2 molecules and lithium diffusion or lithium nickelate phase evolution have not started. The corresponding k values are presented in Table 1. In general, k values tended to increase as a function of temperature, although there was not a linear trend. Differences observed in the k values may be related to temperature-$LiNiO_2$ sintering and/or structural evolution. In any case, it must be imply different activation energies at each temperature.

Finally, if these k values are compared to kinetic data of other alkaline ceramics, it can be seen that k values of $LiNiO_2$ are not so different to Na_2ZrO_3 [57,58] and $NaCoO_2$ [41], where their reported k values around of 0.001–0.002 and 0.001–0.006 s^{-1}, respectively. Consequently, these data show that CO_2 chemisorption on $LiNiO_2$ is kinetically similar than other alkaline ceramics, although this ceramic present a more complex structural and thermal reaction evolution.

4. Conclusions

$LiNiO_2$ was produced via lithium excess method and the structural and microstructural characterizations were performed by XRD, SEM, N_2 adsorption-desorption and different thermal analyses (thermogravimetric and differential thermal analyses). CO_2 chemisorption on $LiNiO_2$ was evaluated using thermogravimetric (dynamic and isothermal) analysis, where carbonated-$LiNiO_2$ products were re-characterized using XRD. The $LiNiO_2$ dynamic curve, in a CO_2 flow, exhibited an atypical behavior in comparison to other alkaline ceramics. This material showed a triple weight increment (200–390, 445–650 and 660–850 °C), which were attributed to CO_2 superficial reactions on $LiNiO_2$ and $Li_{1-x}NiO_2$ phases and the CO_2 bulk chemisorption. It must be mentioned that $LiNiO_2$ phase transformation to $Li_{1-x}NiO_2$ induces some lithium and/or oxygen atoms rearrange, activating a second superficial process. Additionally, $LiNiO_2$ carbonation presented a higher thermal stability ($T \geq 720$ °C), attributed to the formation and thermal stability of $Li_{0.4}Ni_{1.6}O_2$ phase.

The isothermal analysis confirmed the CO_2 chemisorption and a successive $LiNiO_2$ structural evolution. $LiNiO_2$ composition and structure evolved as a function of temperature and lithium reactivity as follows: $LiNiO_2 \rightarrow Li_{0.95}Ni_{1.05}O_2 \rightarrow Li_{0.92}Ni_{1.08}O_2 \rightarrow Li_{0.79}Ni_{1.21}O_2 \rightarrow Li_{0.4}Ni_{1.6}O_2$, in addition to the corresponding amounts of Li_2CO_3 and NiO (between 400 and 500 °C). In fact, the thermal stability observed in this system was associated to previous reports, where it has been established that lithium nickelate produces lithium vacancies. In these cases, some Ni^{3+} atoms move to Li^{1+} crystalline positions as Ni^{2+}, with the consequent O^{2-} release. These results were complemented by a lithium coefficient analysis of lithium nickelate phases, where these results were in very good agreement with the carbonation isothermal trends. Finally, the kinetic constant values (k) obtained for the $LiNiO_2$-CO_2 reaction mechanism tends to increase as a function of temperature, although they did not follow a linear trend due to $LiNiO_2$ sintering and structural evolutions.

Table 1
k values obtained from the first order reaction model during the $LiNiO_2$ carbonation process.

Temperature (°C)	k (s^{-1})	R^2
500	0.0013	0.9798
525	0.0012	0.9962
600	0.0016	0.9915
650	0.0030	0.9974
700	0.0029	0.9984
750	0.0058	0.9970
800	0.0051	0.9948

Acknowledgements

This work was financially supported by the project PAPIIT-UNAM (IN-101916). Authors thank Adriana Tejeda and Josue Romero-Ibarra for technical help.

References

[1] Yancheshmeh MS, Radfarnia HR, Iliuta MC. High temperature CO_2 sorbents and their application for hydrogen production by sorption enhanced steam reforming process. Chem Eng J 2016;283:420–44.
[2] Wang S, An C, Zhang QH. Syntheses and structures of lithium zirconates for high-temperature CO_2 absorption. J Mater Chem A 2013;1:3540–50.
[3] Xiao Q, Liu Y, Zhong Y, Zhu W. A citrate sol–gel method to synthesize Li_2ZrO_3 nanocrystals with improved CO_2 capture properties. J Mater Chem 2011;21:3838–42.
[4] Ochoa-Fernandez E, Zhao T, Ronning M, Chen D. Effects of steam addition on the properties of high temperature ceramic CO_2 acceptors. J Environ Eng 2009;135:397–402.
[5] Nakagawa K. A Novel method of CO_2 capture from high temperature gases. J Electrochem Soc 1998;145:1344–7.
[6] Pfeiffer H, Bosch P. Thermal stability and high-temperature carbon dioxide sorption on hexa-lithium zirconate ($Li_6Zr_2O_7$). Chem Mater 2005;17:1704–10.
[7] Díaz-Herrera PR, Ramírez-Moreno MJ, Pfeiffer H. The effects of high-pressure on the chemisorption process of CO_2 on lithium oxosilicate (Li_8SiO_6). Chem Eng J 2015;264:10–5.
[8] Durán-Muñoz F, Romero-Ibarra IC, Pfeiffer H. Analysis of the CO_2 chemisorption reaction mechanism in lithium oxosilicate (Li_8SiO_6): a new option for high-temperature CO_2 capture. J Mater Chem A 2013;1:3919–27.
[9] Ávalos-Rendón T, Casa-Madrid J, Pfeiffer H. Thermochemical capture of carbon dioxide on lithium aluminates ($LiAlO_2$ and Li_5AlO_4): a new option for the CO_2 absorption. J Phys Chem A 2009;113:6919–23.
[10] Ávalos-Rendón T, Lara VH, Pfeiffer H. CO_2 chemisorption and cyclability analyses of lithium aluminate polymorphs (α-and β-Li_5AlO_4). Ind Eng Chem Res 2012;51:2622–30.
[11] Kim H, Jang HD, Choi M. Facile synthesis of macroporous Li_4SiO_4 with remarkably enhanced CO_2 adsorption kinetics. Chem Eng J 2015;280:132–7.
[12] Zhang Q, Peng D, Zhang S, Ye Q, Wu Y, Ni Y. Behaviors and kinetic models analysis of Li_4SiO_4 under various CO_2 partial pressures. AIChE J 2017;6:2153–64.
[13] Romero-Ibarra IC, Ortiz-Landeros J, Pfeiffer H. Microstructural and CO_2 chemisorption analyses of Li_4SiO_4: effect of surface modification by the ball milling process. Thermochim Acta 2013;567:118–24.
[14] Seggiani M, Puccini M, Vitolo S. High-temperature and low concentration CO_2 sorption on Li_4SiO_4 based sorbents: study of the used silica and doping method effects. Int. J. Greenh. Gas Control 2011;5:741–8.
[15] Gauer C, Heschel W. Doped lithium orthosilicate for absorption of carbon dioxide. J Mater Sci 2006;41:2405–9.
[16] Amorim SM, Domenico MD, Dantas TLP, José HJ, Moreira RFPM. Lithium orthosilicate for CO_2 capture with high regeneration capacity: kinetic study and modeling of carbonation and decarbonation reactions. Chem Eng J 2016;283:388–96.
[17] Duan Y, Pfeiffer H, Li B, Romero-Ibarra IC, Sorescu DC, Luebke DR. CO_2 capture properties of lithium silicates with different ratios of Li_2O/SiO_2: an ab initio thermodynamic and experimental approach. Phys Chem Chem Phys 2013;15:13538–58.
[18] Matsukura Y, Okumura T, Kobayashi R, Oh-ishi K. Synthesis and CO_2 absorption properties of single-phase Li_2CuO_2 as a CO_2 absorbent. Chem Lett 2010;39:966–7.
[19] Palacios-Romero LM, Pfeiffer H. Lithium cuprate (Li_2CuO_2): a new possible ceramic material for CO_2 chemisorption. Chem Lett 2008;37:862–3.
[20] Oh-ishi K, Matsukura Y, Okumura T, Matsunaga Y, Kobayashi R. Fundamental research on gas–solid reaction between CO_2 and Li_2CuO_2 linking application for solid CO_2 absorbent. J Solid State Chem 2014;211:162–9.
[21] Lara-García HA, Alcántar-Vázquez B, Duan Y, Pfeiffer H. CO chemical capture on lithium cuprate, through a consecutive CO oxidation and chemisorption bifunctional process. J. Phys. Chem. C 2016;120:3798–806.
[22] Meng F, Liu Y, Xue T, Su Q, Wang W, Qi T. Structures, formation mechanisms, and ion exchange properties of α–,β-, and γ-Na_2TiO_3. RSC Adv 2016;6:112625–33.
[23] Xu YH, Zhao SX, Deng YF, Deng H, Nan CW. Improved electrochemical performance of 5 V spinel $LiNi_{0.5}Mn_{1.5}O_4$ microspheres by F-doping and Li_4SiO_4 coating. J Mater 2016;2:265–72.
[24] Yan D, Geng X, Zhao Y, Lin X, Liu X. Phase relations of Li_2O–FeO–SiO_2 ternary system and electrochemical properties of $Li_xSi_yO_z$ compounds. J Mater Sci 2016;51:6452–63.

[25] Xiao R, Li H, Chen L. Candidate structures for inorganic lithium solid-state electrolytes identified by high-throughput bond-valence calculations. J Materiomics 2015;1:325–32.
[26] Huang S, Fang Y, Wang B, Wilson BE, Tran N, Truhlar DG, et al. Conduction and surface effects in cathode materials: Li_8ZrO_6 and doped Li_8ZrO_6. J. Phys. Chem. C 2016;120:9637–49.
[27] Khokhani M, Khomane RB, Kulkarni BD. Sodium-doped lithium zirconate nano squares: synthesis, characterization and applications for CO_2 sequestration. J Sol Gel Sci Technol 2012;61:316–20.
[28] Subha PV, Nair BN, Hareesh P, Mohamed AP, Yamaguchi T, Warrier KGK. Enhanced CO_2 absorption kinetics in lithium silicate platelets synthesized by a sol–gel approach. J Mater Chem A 2014;2:12792–9.
[29] Radfarnia HR, Iliuta MC. Surfactant-template/ultrasound-assisted method for the preparation of porous nanoparticle lithium zirconate. Ind Eng Chem Res 2011;50:9295–305.
[30] Jeoung S, Lee JH, Kim HY, Moon HR. Effects of porous carbon additives on the CO_2 absorption performance of lithium orthosilicate. Thermochim Acta 2016;637:31–7.
[31] Xiang M, Zhang Y, Hong M, Liu S, Zhang Y, Liu H. CO_2 absorption properties of Ti- and Na-doped porous Li_4SiO_4 prepared by a sol–gel process. J Mater Sci 2015;50:4698–706.
[32] Ortiz-Landeros J, Gómez-Yáñez C, Palacios-Romero LM, Lima E, Pfeiffer H. Structural and thermochemical chemisorption of CO_2 on $Li_{4+x}(Si_{1-x}Al_x)O_4$ and $Li_{4-x}(Si_{1-x}V_x)O_4$ solid solutions. J Phys Chem A 2012;116:3163–71.
[33] Aceves-Olivas DY, Baray-Guerrero MR, Escobedo-Bretado MA, Marques da-Silva PM, Salinas-Gutiérrez J, Guzmán-Velderrain V. Enhanced ethanol steam reforming by CO_2 absorption using CaO, CaO*MgO or Na_2ZrO_3. Int J Hydrogen Energy 2014;39:16595–607.
[34] Chen Y, Zhao Y, Zhang J, Zheng C. Hydrogen production through CO_2 sorption-enhanced methane steam reforming: comparison between different adsorbents. Sci China Technol Sci 2011;54:2999–3008.
[35] Essaki K, Muramatsu T, Kato M. Effect of equilibrium-shift in the case of using lithium silicate pellets in ethanol steam reforming. Int J Hydrogen Energy 2008;33:6612–8.
[36] Halabi MH, de-Croon MHJM, van der Schaaf J, Cobden PD, Schouten JC. Reactor modeling of sorption-enhanced autothermal reforming of methane. Part I: performance study of hydrotalcite and lithium zirconate-based processes. Chem Eng J 2011;168:872–82.
[37] Ochoa-Fernández E, Rusten HK, Jakobsen HA, Rønning M, Holmen A, Chen D. Sorption enhanced hydrogen production by steam methane reforming using Li_2ZrO_3 as sorbent: sorption kinetics and reactor simulation. Catal Today 2005;106:41–6.
[38] Ochoa-Fernández E, Haugen G, Zhao T, Rønning M, Aartun I, Børresen B. Process design simulation of H_2 production by sorption enhanced steam methane reforming: evaluation of potential CO2 acceptors. Green Chem 2007;9:654–61.
[39] Mendoza-Nieto JA, Vera E, Pfeiffer H. Methane reforming process by means of a carbonated-Na_2ZrO_3 catalyst. Chem Lett 2016;86:3–6.
[40] Royer S, Duprez D. Catalytic oxidation of carbon monoxide over transition metal oxides. ChemCatChem 2011;3:24–65.
[41] Vera E, Alcántar-Vázquez B, Pfeiffer H. CO_2 chemisorption and evidence of the CO oxidation–chemisorption mechanisms on sodium cobaltate. Chem Eng J 2015;271:106–13.
[42] Alcántar-Vázquez B, Vera E, Buitron-Cabrera F, Lara-García HA, Pfeiffer H. Evidence of CO oxidation–chemisorption process on sodium zirconate (Na_2ZrO_3). Chem Lett 2015;44:480–2.
[43] Kalyani P, Kalaiselvi N. Various aspects of $LiNiO_2$ chemistry: a review. Sci Technol Adv Mater 2005;6:689–703.
[44] Arai H, Okada S, Sakurai Y, Yamaki J. Reversibility of $LiNiO_2$ cathode. Solid State Ionics 1997;95:275–82.
[45] Lin SP, Fung KZ, Hon YM, Hon MH. Crystallization mechanism of $LiNiO_2$ synthesized by Pechini method. J Cryst Growth 2001;226:148–57.
[46] Lowell S, Shields JE, Thomas MA, Thommes M. Characterization of porous solids and powders: surface area, pore size and density. London: Particle Technology Series, Kluwer Academic Publishers; 2004.
[47] Bretado ME, Guzmán-Velderrain V, Lardizábal-Gutiérrez D, Collins-Martínez V, Ortiz AL. A new synthesis route to Li_4SiO_4 as CO_2 catalytic/sorbent. Catal Today 2005;107–108:863–7.
[48] Iwan A, Stephenson H, Ketchie WC, Lapkin AA. High temperature sequestration of CO_2 using lithium zirconates. Chem Eng J 2009;146:249–58.
[49] Nair BN, Burwood RP, Goh VJ, Nakagawa K, Yamaguchi T. Lithium based ceramic materials and membranes for high temperature CO_2 separation. Prog Mater Sci 2009;54:511–41.
[50] Yin XS, Zhang QH, Yu JG. Three-step calcination synthesis of high-purity Li_8ZrO_6 with CO_2 absorption properties. Inorg Chem 2011;50:2844–50.
[51] Ortiz-Landeros J, Ávalos-Rendón TL, Gómez-Yánez C, Pfeiffer H. Analysis and perspectives concerning CO_2 chemisorption on lithium ceramics using thermal analysis. J Therm Anal Calorim 2012;108:647–55.
[52] Wang K, Guo X, Zhao P, Wang F, Zheng C. High temperature capture of CO_2 on lithium-based sorbents from rice husk ash. J Hazard Mater 2011;189:301–7.
[53] Mosqueda HA, Vazquez C, Bosch P, Pfeiffer H. Chemical sorption of carbon dioxide (CO_2) on lithium oxide (Li_2O). Chem Mater 2006;18:2307–10.
[54] Bhatta LKG, Subramanyam S, Chengala MD, Olivera S, Venkatesh K. Progress in hydrotalcite like compounds and metal-based oxides for CO_2 capture: a review. J Clean Prod 2015;103:171–96.
[55] Xiao Q, Tang X, Liu Y, Zhong Y, Zhu W. Citrate route to prepare K-doped Li_2ZrO_3 sorbents with excellent CO_2 capture properties. Chem Eng J 2011;174:231–5.
[56] Molenda J, Wilk P, Marzec J. Structural, electrical and electrochemical properties of $LiNiO_2$. Solid State Ionics 2002;146:73–9.
[57] Alcérreca-Corte I, Fregoso-Israel E, Pfeiffer H. CO_2 absorption on Na_2ZrO_3: a kinetic analysis of the chemisorption and diffusion processes. J. Phys. Chem. C 2008;112:6520–5.
[58] Martínez-dlCruz L, Pfeiffer H. Cyclic CO_2 chemisorption–desorption behavior of Na_2ZrO_3: structural, microstructural and kinetic variations produced as a function of temperature. J Solid State Chem 2013;204:298–304.

Daniela González-Varela studies a master's degree in Chemistry Sciences at the Universidad Nacional Autónoma de México (UNAM), where she previously studied Chemistry. During her Bachelor's thesis, she worked on the CO_2 capture process, using lithium nickelate as a high temperature ceramic captor.

Brenda Alcántar-Vázquez is, currently, a postdoctoral fellow at the Engineering Institute, Universidad Nacional Autónoma de México (UNAM). She obtained a Ph D from the Universidad Autónoma de Baja California in 2014 and she occupied a postdoctoral position at the Materials Research Institute UNAM between 2014 and 2015. Recently, she has been working with different bifunctional materials (CO oxidants and subsequently CO_2 captors) as possible syngas separation systems and also about the valorization of wastes and byproducts as sorbents and catalysts for remove air pollutants. Her research interests involve gas sorption processes, catalysis, green chemistry and different structural and microstructural techniques.

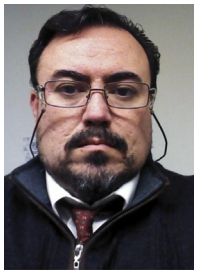

Heriberto Pfeiffer works on different sorption and catalytic processes, having more than 120 papers published and 5 book chapters (h-index = 22). His research is focused on CO_2 capture and its possible conversion to added value products. At the same time, Heriberto works on different reforming and other catalytic processes, as well as on the CO oxidation-chemisorption process as a possible syngas separation. Additionally, he is interested in high temperature dense membranes for CO_2 separation. Finally, Heriberto Pfeiffer works in biodiesel production and glycerol conversion.